

# Electronic and structural properties of superconducting diborides and calcium disilicide in the AlB<sub>2</sub> structure

G. Satta<sup>†</sup>, G. Profeta\*, F. Bernardini<sup>†</sup>, A. Continenza\* and S. Massidda<sup>†</sup>

\**Istituto Nazionale di Fisica della Materia (INFM) and Dipartimento di Fisica, Università degli Studi di L’Aquila, I-67010 Coppito (L’Aquila), Italy*

<sup>†</sup>*Istituto Nazionale di Fisica della Materia (INFM) and Dipartimento di Fisica Università degli Studi di Cagliari, 09124 Cagliari, Italy*

## Abstract

We report a detailed study of the electronic and structural properties of the 39K superconductor MgB<sub>2</sub> and of several related systems of the same family, namely Mg<sub>0.5</sub>Al<sub>0.5</sub>B<sub>2</sub>, BeB<sub>2</sub>, CaSi<sub>2</sub> and CaBe<sub>0.5</sub>Si<sub>1.5</sub>. Our calculations, which include zone-center phonon frequencies and transport properties, are performed within the local density approximation to the density functional theory, using the full-potential linearized augmented plane wave (FLAPW) and the norm-conserving pseudopotential methods. Our results indicate essentially three-dimensional properties for these compounds; however, strongly two-dimensional  $\sigma$ -bonding bands contribute significantly at the Fermi level. Similarities and differences between MgB<sub>2</sub> and BeB<sub>2</sub> (whose superconducting properties have not been yet investigated) are analyzed in detail. Our calculations for Mg<sub>0.5</sub>Al<sub>0.5</sub>B<sub>2</sub> show that metal substitution cannot be fully described in a rigid band model. CaSi<sub>2</sub> is studied as a function of pressure, and Be substitution in the Si planes leads to a stable compound similar in many aspects to diborides.

PACS numbers: 74.25.jb, 74.70.-b, 74.10.+v, 71.20.-b

## I. INTRODUCTION

The recent discovery [1] of superconductivity at  $\approx 39\text{K}$  in the simple intermetallic compound  $\text{MgB}_2$  is particularly interesting for many reasons. In the first instance, this critical temperature is by far the highest if we exclude oxides and  $\text{C}_{60}$  based materials. Furthermore, B isotope effect [1] indicates that  $\text{MgB}_2$  may be a BCS phonon-mediated superconductor, with  $T_c$  above the commonly accepted limits for phonon-assisted superconductivity. Another reason of interest is that the  $\text{AlB}_2$ -type structure of  $\text{MgB}_2$  (which can be viewed as an intercalated graphite structure with full occupation of interstitial sites centered in hexagonal prisms made of B atoms) is shared by a large class of compounds (more than one hundred), where the B site can be occupied by Si or Ge, but also by Ni, Ga, Cu, Ag, Au, Zn and Cd, and Mg can be substituted by divalent or trivalent  $sp$  metals, transition elements or rare earths. Such a variety is therefore particularly suggestive of a systematic study. To confirm this interest, a recent study [2] showed that superconductivity is suppressed by addition of more than about 30% of Al atoms. Pressure effects [3] also lead to a depression of superconductivity.

While claims [4] of very high temperature superconductivity in diborides were never confirmed, superconductivity at  $T_c \approx 14\text{K}$  was observed in disilicides. Recent experimental work has in fact pointed out that pressure can be effectively used to tune both structural and physical properties of the metal silicon compound  $\text{CaSi}_2$  [5,6]. In particular, Bordet and co-workers [5] identified a new structural phase transition for  $\text{CaSi}_2$  from trigonal to hexagonal  $\text{AlB}_2$ -type structure, with superconductivity at  $T_c = 14\text{ K}$ , one of the highest transition temperatures known for a silicon based compound. The occurrence of this structural phase transition implies that Si shifts from  $sp^3$  to  $sp^2$  hybridization, and experiment points to a clear enhancement of  $T_c$  when going from an  $sp^3$  to an  $sp^2$  environment [5]. The temperature dependence of the Hall coefficient observed in  $\text{CaSi}_2$  indicates that this compound is a compensated metal for which electrons and holes contribute in an equivalent way to the conductivity [7], in qualitative agreement with electronic structure calculations.

Early studies [8–10] of the electronic structure of diborides by the OPW and tight-binding methods have shown similarity with graphite bands. A more systematic study of  $\text{AlB}_2$ -type compounds [12,13] by the full-potential LAPW method showed in simple metal diborides the presence of interlayer states, similar to those previously found in graphite [14,15], in addition to graphite-like  $\sigma$  and  $\pi$  bands. Transition metal diborides, on the other hand, show a more complex band structure due to the metal  $d$  states. A very recent electronic structure calculation [16] on  $\text{MgB}_2$  shows that metallicity is due to B states. Phonon frequencies and electron-phonon couplings (at the  $\Gamma$  point) lead these authors to suggest phonon-based superconductivity. Further, new calculations [17] on related compounds ( $\text{LiB}_2$  and graphitic-like B) addressed the peculiar contributions to conductivity coming from the interplay of 2D and 3D Fermi surface features. An alternative mechanism has been proposed by Hirsch [11], based on dressed hole carriers in the B planes, in the presence of almost filled bands. As for the silicides, many electronic structure studies have been carried out for the different phases [18–20], while the  $\text{AlB}_2$ -type structure of  $\text{CaSi}_2$  was first studied by Kusakabe et al. [21], before its actual synthetization.

As previously pointed out, this family of compounds provides a wide playground for the search of new superconductors, and we intend to provide here a contribution, based on a de-

tailed study of electronic and structural properties together with phonon spectra, for several  $\text{AlB}_2$ -type compounds and for  $\text{CaSi}_2$ , in the trigonal and hexagonal structures. The questions that we want to address are the following: (i) how do the electronic properties of  $\text{MX}_2$  depend on the atomic species M; namely, can rigid band schemes provide the correct trend, or is the metal effect mostly mediated by lattice parameter changes (chemical pressure). (ii) Ref. [16] shows the presence of both B  $\pi$  Fermi surfaces (FS) giving rise to 3-dimensional states, and of small 2-dimensional B  $\sigma$ -bonding pockets. It is of course interesting to know which of the FS is mostly involved with superconductivity. The trends observed in the band structures, together with experimental studies, will contribute to elucidate this point. In the same way, changes in the Fermi level density of states with chemical composition will possibly correlate with  $T_c$  values. (iii) Pure  $\text{CaSi}_2$  shows a trigonal instability, joined by a buckling of  $\text{Si}_2$  planes, which is apparently [5] strongly reduced under high pressure, or by Be substituting some of the Si sites. The presence, or the proximity, of structural instabilities (investigated through phonon spectra), will hopefully provide hints to further experimental search of new materials.

In this paper, we present calculations for  $\text{MgB}_2$ ,  $\text{Mg}_{0.5}\text{Al}_{0.5}\text{B}_2$ ,  $\text{BeB}_2$ ,  $\text{CaSi}_2$  and  $\text{CaBe}_x\text{Si}_{2-x}$  ( $x = 1$ ), based on the local density approximation (LDA) to the density functional theory. We use both the Full Linearized Augmented Plane Wave [22] method, and the norm-conserving pseudopotential method. In Sec. II we give some computational detail; in Sect. III we discuss the electronic properties for all the compounds considered; we finally draw our conclusion in Sect. IV.

## II. COMPUTATIONAL AND STRUCTURAL DETAILS

Our calculations were performed using the “all-electron” full potential linearized augmented plane waves (FLAPW) [22] method, in the local density approximation (LDA) to the density functional theory. In the interstitial region we used plane waves with wave vector up to  $K_{max} = 3.9$  a.u. and 4.1 a.u. for disilicides and diborides, respectively (we used the larger  $K_{max} = 4.4$  a.u. for  $\text{BeB}_2$  because of the smaller spheres imposed by the smaller lattice parameters). Inside the muffin tin spheres, we used an angular momentum expansion up to  $l_{max} = 6$  for the potential and charge density and  $l_{max} = 8$  for the wave functions. The Brillouin zone sampling was performed using the special  $k$ -points technique according to the Monkhorst-Pack scheme [23], and also the linear tetrahedra method up to 60  $k$ -points in the irreducible Brillouin zone. We used muffin tin radii  $R_{MT} = 2.2, 1.8, 1.59$  and 2.1 a.u., for Ca, Si, B, and the remaining elements respectively (we used  $R_{Be} = 2$  a.u. and  $R_B = 1.5$  a.u. in  $\text{BeB}_2$ ).

The crystallographic structure of  $\text{AlB}_2$  (C32) is hexagonal, space group  $P6mmm$  with graphitic B planes, and 12-fold B-coordinated Al atoms sitting at the center of B hexagonal prisms. The unit cell contains one formula unit, with Al atom at the origin of the coordinates and two B atoms in the positions ( $\mathbf{d}_1 = (a/2, a/2\sqrt{2}, c/2)$ ,  $\mathbf{d}_2 = -\mathbf{d}_1$ ). The trigonal distortion in  $\text{CaSi}_2$  corresponds to a buckling of Si planes leading to a  $P3\bar{m}1$  space group symmetry ), with one internal order parameter  $z$  - being  $z = 0.5$  the value corresponding to the  $\text{AlB}_2$  structure.

Phonon frequencies were computed using the ABINIT code [24] by means of Linear Response Theory [25,26] (LRT) approach in the framework of pseudopotentials plane wave

method [24]. Troullier and Martins [27] soft norm-conserving pseudopotentials were used for all the elements considered, Mg and Ca  $p$  semicore states were not included in the valence, their contribution to the exchange and correlation potential was accounted by the non-linear core corrections [28]. The local density approximation to the exchange-correlation functional is used. A plane wave cutoff of 44 Ry was found sufficient to converge structural properties of the compounds. Brillouin zone integration was performed using a  $12 \times 12 \times 12$  Monkhorst-Pack [23] mesh. To improve  $k$ -point sampling convergence a gaussian smearing with an electronic temperature of 0.04 Ha was used. Experimental lattice constant were used in the ground state and LRT calculations.

### III. ELECTRONIC AND STRUCTURAL PROPERTIES

#### A. Diborides

We shall start our discussion of electronic properties of diborides by presenting in Fig. 1 the energy bands of the superconducting compound  $\text{MgB}_2$ , which will be the reference for all our further studies (the  $M - \Gamma - K$  lines are in the basal plane, while the  $L - A - H$  lines are the corresponding ones on the top plane at  $k_z = \pi/c$ ). We used the experimental lattice parameters  $a = 3.083\text{\AA}$ ,  $c = 3.52\text{\AA}$ . Our results, which are in excellent agreement with those of Kortus et. al. [16], show strong similarities with the band structures of most simple-metal diborides [12], computed by the FLAPW method. They show strongly bonded  $sp^2$  hybrids laying in the horizontal hexagonal planes, forming the three lowest ( $\sigma$ -bonding) bands, as the main structure in the valence region. The corresponding antibonding combinations are located around 6 eV above the Fermi level ( $E_F$ ).

The bonding along the vertical direction is provided by the  $\pi$  bands (at  $\sim -3$  eV and  $\sim 2$  at  $\Gamma$ ), forming the double bell-shaped structures. Similarly to  $\text{AlB}_2$ -type diborides, and unlike graphite, we notice a large dispersion of the  $\pi$  bands along the  $k_z$  direction ( $\Gamma - A$ ). This can be understood on a tight-binding approach: the phases of the Bloch functions lead the B  $p_z$  orbitals on adjacent layers to be antibonding at  $\Gamma$ , and bonding at  $A$ . The downwards dispersion of the  $\pi$ -bonding band (from  $-3$  to  $-7$  eV along  $\Gamma - A$ ) is joined by an opposite upwards dispersion of an empty band, (at  $\approx 2$  eV at the  $\Gamma$  point) which is a direct indication of the strong interaction among these states. The analysis of the wavefunctions for this empty band reveals that this band has an interstitial character ( $\approx 64\%$  of its charge is located in the interstitial region), and is very similar to those found in graphite [15], in diborides [12], in  $\text{CaGa}_2$  [13], but also in  $\text{CaSi}_2$ . In fact, this band is missing in atomic-orbitals only based tight-binding calculations [10], and has been shown [12] to be present even in hypothetical compounds completely deprived of intercalated metal atoms. A general description of the bonding can be given by the partial density of states (PDOS), shown in Fig. 2. The B PDOS, in particular, shows bonding and antibonding structures for the  $s$  and  $p$  states. The  $p_z$  states give rise to a rather wide structure responsible for less than half of the DOS at  $E_F$ , which therefore results having predominantly B  $p - \sigma$  character.

In the search of similar materials having the desired superconducting properties,  $\text{BeB}_2$  is the first natural candidate, as the band filling is expected to be pretty similar, and lighter Be atoms may help providing larger phonon frequencies while keeping similar electronic properties. The only experimental report [29] on  $\text{BeB}_2$ , to our knowledge, gives the average

lattice constants. These parameters have been used for all the previous calculations of the  $\text{BeB}_2$  [9,12]. We have optimized the lattice constants, obtaining  $a = 2.87\text{\AA}$ ,  $c = 2.85\text{\AA}$ , smaller than in  $\text{MgB}_2$  and similar to the values estimated by the average experimental values. In particular, we notice that while  $a$  reduces only by about 7.4%,  $c$  reduces by about 24% when Mg is substituted by Be, a result which can be understood pretty easily. On one hand, in fact, the optimization of  $\sigma$ -bonds prevents a too drastic variation of the  $a$  parameter; on the other hand,  $c$  can change more easily as the vertical bonding, provided by the  $\pi$  bands, has a large contribution from the metal orbitals. The band structure of  $\text{BeB}_2$ , shown in Fig 3, are pretty similar to those computed by the FLAPW method [12] at the experimentally estimated lattice parameters. We can remark the strong similarities with the  $\text{MgB}_2$  compound, which includes the presence of  $\sigma$ -bonding hole pockets along  $\Gamma - A$ , but also a few relevant differences. First of all, the shorter lattice parameters lead to wider valence bands, and also to more dispersed  $\sigma$  bands, in particular the cylindrical hole pocket along  $\Gamma - A$ , which might be relevant for superconductivity. Also, the different energy location of the metal  $s$ -free electron band (lower in  $\text{MgB}_2$ ), and the different shape of the  $\pi$ -bonding band (related by the different  $c$  values) causes a different occupation of this band, especially along  $\Gamma - M$ .

To further investigate these two materials, we studied the zone center phonon frequencies of  $\text{MgB}_2$  and  $\text{BeB}_2$ , using the linear response approach, with the pseudopotential method; calculations have been carried out at the experimental lattice constant. Our results are listed in Table I. The two lowest independent frequencies correspond to a motion of the intercalated metal atoms relative to the rigid B networks: one vertical mode ( $A_{2u}$ ), and one doubly degenerate in-plane mode, ( $E_{1u}$ ). The two higher frequencies represent the internal motion of the B network itself: again one vertical mode ( $B_{1g}$ ), now representing a trigonal distortion producing a buckling of the planes similar to that found in  $\text{CaSi}_2$ , and one degenerate ( $E_{2g}$ ) mode giving an in-plane stretching of B-B bonds. Our calculations for  $\text{MgB}_2$  are in reasonable agreement with those of Kortus et al. [16], apart from the  $E_{2g}$  frequency, higher in our calculation. This discrepancy may be due to the different computational schemes used, as well as to the use of the experimental lattice constant, probably differing more from the equilibrium value within pseudopotential than FLAPW method. The comparison between the two compounds shows a much higher  $E_{2g}$  frequency in  $\text{BeB}_2$ . Surprisingly, however, two of the remaining frequencies are lower in  $\text{BeB}_2$ , namely the  $A_{2u}$  mode which involves the motion of lighter Be atoms against the B network and the  $B_{1g}$  mode. This indicates a strong dependence of the phonon spectra of these materials on the electronic structure details. The lowest  $E_{1u}$  mode has comparable frequencies.

The states at the Fermi level, responsible for superconductivity, show two different orbital characters:  $p - \sigma$  bonding (column-like FS around  $\Gamma - A$ ) and  $p_z$ , having  $\pi$ -bonding and antibonding character on the basal and on the top ( $k_z = \pi/c$ ) planes, respectively. Which one of them is the most important for superconductivity is not yet known. A very recent experimental report by Slusky et al. [2] shows that Al doping destroys bulk superconductivity when the Al content  $x$  is greater than  $\approx 0.3$ . Stimulated by these results, we studied the chemical substitution of Mg with Al. The substitution corresponding to a 50% concentration of Al ( $x = 0.5$ ) leads to a reduction of the cell parameters, from  $a = 3.083\text{\AA}$ ,  $c = 3.521\text{\AA}$  [30] for  $\text{MgB}_2$ , to  $a = 3.047\text{\AA}$ ,  $c = 3.366\text{\AA}$  [30] for  $\text{Mg}_{0.5}\text{Al}_{0.5}\text{B}_2$ . These differences again indicate hardly compressible B-B  $\sigma$  bonds, and interlayer distances quite

sensitive to the intercalated cation. The study of Slusky et al. [2] shows consistent results, and indicates, furthermore, that after a two-phases region for Al substitutions from 10 to 25%,  $c$  collapses and bulk superconductivity disappears. We first studied this problem in a rigid band approach, bringing  $\text{MgB}_2$  to the same lattice parameters of  $\text{Al}_{0.3}\text{Mg}_{0.7}\text{B}_2$  [2]. The only apparent change at that electron concentration is the complete filling of the  $\pi$  bonding band at the  $M$  point. The  $\sigma$  bonding bands need a larger electron addition to be completely filled in a rigid band model.

To investigate further this problem, we studied the system with 50% Al concentration. We used in our calculations the experimental values, and in a first approach simulated the disorder (certainly present in the real compound) using an orthorhombic supercell, containing two formula units. We started by calculating the energy bands using the  $\text{MgB}_2$  lattice constants, and then we used the experimental  $\text{Mg}_{0.5}\text{Al}_{0.5}\text{B}_2$  constants. The results of these calculations are shown in Fig. 4 together with the bands of  $\text{MgB}_2$ , folded into the Brillouin zone (BZ) of the orthorhombic structure. The folding is such that the  $\Gamma$  point of the orthorhombic BZ corresponds to the  $\Gamma$  and  $M$  points of the hexagonal BZ, while  $Z$  corresponds to both the hexagonal  $A$  and  $L$ . Therefore, the  $\Gamma - Z$  line collects the  $\Gamma - A$  and the  $M - L$  hexagonal lines, and we notice immediately the three  $\pi$  bands (two bonding and one anti-bonding, coming from folding). The  $\Gamma - X$  line contains the (folded) hexagonal  $\Gamma - M$  line. If we first look at the frozen structure calculation Fig. 4(c), we see quite similar band dispersions with the obvious splittings, related to the symmetry lowering induced by the different cations, and a different band filling. We notice, however, a lowering of the folded  $\pi$  antibonding band, related to the different cations: the  $\pi$  band is in fact pushed downwards by the interaction with the free-electron metal- $s$  band, which is at lower energy in the compounds with Al (this band is partially filled in pure, non superconducting,  $\text{AlB}_2$  [12]). As a consequence, the extra electrons coming from Al do not fill the  $\sigma$ -bonding band completely, leaving hole pockets around  $Z$ . As we relax the structure, the  $\sigma$  bands increase their width due to the smaller  $a$  value, and the situation near  $E_F$  changes only because of the occupation of the free-electron band around  $\Gamma$ . These results suggest that although the rigid band scheme can be considered roughly correct, the dependence upon doping of the physical properties and of Fermi surface states relevant for superconductivity, may be crucially dependent on the actual substitutional atom.

We have computed, within a rigid band scheme and using the scheme described, e.g., in Ref. [31], the Fermi velocities, plasma frequencies (along the principal axes of the crystal), and the independent components of the Hall tensor for  $\text{BeB}_2$  and  $\text{MgB}_2$ . Because of hexagonal symmetry, the non-zero components will be  $R_{xyz}$ , corresponding to the magnetic field along the  $z$  axis and transport in plane, and  $R_{zxy} = R_{yzz}$  corresponding to in-plane magnetic field. The results, plotted in Fig. 5 as a function of the hole or electron-type doping, show relatively smooth variations over a wide range of doping, and are nearly coinciding, at zero doping, with the corresponding calculations by Kortus et al. [16]. After comparing the two materials, the following remarks can be done: (i) the density of states at  $E_F$  is smaller in  $\text{BeB}_2$ . (ii)  $\text{MgB}_2$  is nearly isotropic in terms of plasma frequencies and Fermi velocities, while  $\text{BeB}_2$  is expected to show important anisotropy in resistivity, and, in particular, the in-plane conductivity is expected to be smaller. A band-by-band decomposition explains these results in term of very similar (and very anisotropic) contributions in the two compounds from  $\sigma$  states, and quite different contributions from the  $\pi$  bands, nearly isotropic

in  $\text{MgB}_2$  and favoring conductivity along the  $c$ -axis in  $\text{BeB}_2$ . These results point out that despite structural similarity, the electronic properties of  $\text{AlB}_2$ -type structures differ substantially from graphite and intercalation graphite compounds. (iii) The Hall coefficients are positive (hole-like) when the magnetic field is along the  $z$  axis (transport in-plane), while is negative for  $\text{MgB}_2$  and almost zero but negative for  $\text{BeB}_2$ , when the magnetic field is in-plane. A detailed analysis shows again comparable contributions in the two compounds from  $\sigma$  bands, while the sign of  $R_{zxy}$  and  $R_{yxz}$  comes from a balance of the  $\pi$  bands. The Hall coefficient of  $\text{MgB}_2$  has been recently measured by Kang et al. [32].  $R_H$ , which will correspond in this case to an average of the tensor components, turns out to be positive and to decrease with temperature. At  $T = 100\text{K}$  they give  $R_H = 4.1 \times 10^{-11}\text{m}^3/\text{C}$ , and an extrapolation of their results at  $T \rightarrow 0$ , gives  $R_H \approx 6.5 \times 10^{-11}\text{m}^3/\text{C}$ . If we average, at zero doping, our tensor components, the positive contributions overcome the negative ones, resulting in an average value  $R_H \approx 2 \times 10^{-11}\text{m}^3/\text{C}$ . This value is thus of the correct order, but single crystal measurements are probably necessary to have a significant comparison, avoiding an average of quantities with different sign. It is worth noticing that, if the sign of carriers has a role on superconductivity [11],  $\text{BeB}_2$  also has a positive Hall coefficient. Summaryzing this discussion, we see that if superconductivity would turn out to be related to  $\sigma$ -bonding electrons, the two compounds will be basically different (electron-wise) only because of the larger density of states in  $\text{MgB}_2$  which in turn can be ascribed to the different lattice parameters.

## B. Calcium Disilicide

When prepared at ambient pressure  $\text{CaSi}_2$  has a rhombohedral structure (space group  $R3\bar{m}$ ,  $a = 3.85 \text{ \AA}$ ,  $c = 30.62 \text{ \AA}$ ) [33] and is a semimetal [19], not superconducting down to 30 mK [7]. By annealing under pressure - typical condicitions are 4 GPa and 1300 – 1800 K - a tetragonal superconducting ( $\alpha$ - $\text{ThSi}_2$ -type) phase appears with a 3-dimensional network [34] of Si, showing superconducivity with  $T_c = 1.58 \text{ K}$ . At pressures between  $\approx 7 \text{ GPa}$  and  $9.5 \text{ GPa}$  rhombohedral structure samples undergo a transition to a trigonal phase ( $P3\bar{m}1$ ,  $a_T \approx 3.78 \text{ \AA}$ ,  $c_T \approx c_R/6 \approx 4.59 \text{ \AA}$ ) with Si at  $2d$  positions, and  $z = 0.4$ . A second phase transition occurs at 16 GPa. This new phase may be described as [5] an  $\text{AlB}_2$ -type structure with  $z$  slightly smaller than the ideal value  $1/2$ . The transition to the  $\text{AlB}_2$ -type structure implies a switch of the Si bonding from the tetrahedral  $sp^3$  to an almost planar  $sp^2$  coordination. Kusakabe and coworkers [21] have predicted the existence of an  $\text{AlB}_2$ -type polymorph at high pressure. The  $\text{AlB}_2$ -type structure was previously observed in rare-earth silicides [35], while in  $\text{CaSi}_2$  it is apparently stabilized by doping the Si planes with Be [36]. We will discuss this point later. We report electronic structure calculations for the  $\text{AlB}_2$ -type polymorph of  $\text{CaSi}_2$  at the experimental lattice costant, as given by Bordet et al. [5], and we discuss the relative stability of the hexagonal versus trigonal polymorph, after a presentation of the electronic states.

In Fig. 6 we show the energy bands of  $\text{CaSi}_2$  in the  $\text{AlB}_2$  structure (dashed lines), superimposed with those of the trigonal structure (full lines), along the main symmetry lines of the Brillouin zone. Since this polymorph can be obtained only under pressure, we do not minimize the lattice parameters, but rather use the experimental values  $a = 3.7077 \text{ \AA}$  and  $c = 4.0277 \text{ \AA}$ , and optimize the internal parameter  $z$ . The bands in the  $\text{AlB}_2$  structure

show strong similarities with those of simple metal diborides, and of  $\text{CaGa}_2$  [12]. The major difference is provided by Ca  $d$  states, which are mostly found in the conduction region, above 4 eV; however, there is a  $p$ - $d$  mixing between Si and Ca, especially concerning Si  $\pi$  and Ca  $d_{z^2}$  orbitals, also mixing with the free-electron states. Unlike  $\text{MgB}_2$ , the Fermi level of  $\text{CaSi}_2$  cuts the  $\pi$ -antibonding bands over all the Brillouin zone. This of course implies a reduced contribution of  $\pi$  states to the stabilization of an  $sp^2$  environment, consistent with the  $sp^3$ -like trigonal distortion. We will come back to this point later. The energy bands in the trigonal structure show that, a part from a small rigid shift, the  $\sigma$  bands change very little with respect to the  $\text{AlB}_2$  structure. The  $\pi$  bands, on the other hand, show anticrossings which in the antibonding case are located right at the Fermi level. This is most clearly indicated in the density of states of  $\text{CaSi}_2$ , reported in Fig. 7. The dip at  $E_F$  in the trigonal structure provides a textbook explanation for the lattice distortion. While it is tempting to associate the  $T_c$  enhancement in the  $\text{AlB}_2$  structure with the larger density of states at  $E_F$  within a BCS approach, other factors as phonon spectra and electron-phonon couplings will obviously be as important.

In order to understand the stability of  $\text{AlB}_2$ -type polymorph, we study the total energy variation as a function of  $z$ , relative to the ideal  $z = 0.5$  case, for two experimental structures [5], and report it in Fig. 8(a). There is a good agreement between theory and experiment, and a non-negligible ( $\approx 30$  mRy per formula unit) stabilization energy. As we fix  $a$  and  $c$  to the values corresponding to the larger experimental pressure [5], we see much smaller changes in the equilibrium  $z$  than experiments ( $z \sim 0.448$ ), relative to the lower pressure values. This indicates that some different modification might be going on in the experimental samples. In order to assess the stability of this compound in the  $\text{AlB}_2$  structure, and on the light of our previous discussion, we vary the atomic number of cation, which now describes a virtual atom ranging from Ca to K (corresponding to  $Z = 20+x$ ). Our results, reported in Fig 8(b), show that while  $x = -0.3$  leaves the total energy curve almost unchanged,  $x = -0.7$  or larger give a nearly vanishing trigonal stabilization energy. This is consistent with our previous conclusion that a filling of  $\pi$ -antibonding bands destabilizes the  $\text{AlB}_2$  structure. This last conclusion is supported by the existence, in the hexagonal structure, of  $\text{CaBe}_x\text{Si}_{2-x}$ , with  $x = 0.75$ , with  $a = 3.94$  Å and  $c = 4.38$  Å. In fact, Be doping removes electrons from the  $\text{Si}_2$  planes, and brings the formal filling of the above  $\pi$ -antibonding bands to the level found in diborides. To investigate these effects, we studied the (artificially ordered, but existing)  $\text{CaBe}_x\text{Si}_{2-x}$  system for  $x = 1$ , not far from the experimental stoichiometry. The corresponding bands, shown in Fig. 9, have been calculated at the experimental lattice parameters ordering Be and Si atoms as, e.g., in hexagonal BN. In this way, the Brillouin zone is the same as in the undoped compound, and the interpretation is easier. The  $\text{CaBeSi}$  band structure shown are overall similar to that of the undoped compound. The symmetry lowering induced by substitution produces the large splitting of degeneracies at the K and H points. The major difference is of course related to the position of the Fermi level, which is almost exactly coinciding with that found in the superconducting  $\text{MgB}_2$ . The reduced bandwidth for the  $\sigma$  bonding bands may be associated with the smaller size of Be orbitals. The electron depletion from the antibonding  $\pi$ -bands removes the trigonal instability, as demonstrated by total energy calculations. The  $B_{1g}$  mode, corresponding to the trigonal distortion, will therefore be close to an instability in Be-doped calcium disilicide, which may offer an interesting playground in the search of superconducting materials.

While it is difficult to say, on the basis of our electronic structure calculations only, whether the similarities with  $\text{MgB}_2$  band structure can lead to superconductivity, it may be useful to provide hints on the stability of this compound, which may help experimentalists in the search of new compounds. The PDOS in Fig. 10 show a strong hybridization between Si and Be states, in the valence region. In other words, substitutions on the Si site can be possible without disrupting the  $sp^2$  network if one-electron energies of the impurity atoms are comparable with those of Si, and light atoms should be preferred in order to keep high values of phonon frequencies. We may suggest B, which however corresponds to a hole doping smaller than Be.

#### IV. CONCLUSIONS

We have performed electronic structure calculations for  $\text{MgB}_2$ ,  $\text{BeB}_2$ ,  $\text{Mg}_{0.5}\text{Al}_{0.5}\text{B}_2$ ,  $\text{CaSi}_2$  in the trigonal and in the  $Al\text{B}_2$ -type polymorphs at the high pressure experimental structural parameters, and for the  $\text{CaBe}_x\text{Si}_{2-x}$  system ( $x = 1$ ), experimentally stabilized for  $x = 0.75$ . We have calculated band structures, PDOS, transport properties and phonon frequencies, using the FLAPW and the norm-conserving ab-initio pseudopotential methods, within the local density approximation. The following conclusions can be drawn on the basis of our calculations: as compared to  $\text{MgB}_2$ ,  $\text{BeB}_2$  has a similar filling of  $\sigma$  bands, but differs in terms of  $\pi$  states near  $E_F$ . The DOS at  $E_F$  is lower, and some phonon frequencies are substantially higher while others are comparable or lower. It would be interesting to see whether this compound is superconductor, but only one experimental report exists for  $\text{BeB}_2$ . Al substitution cannot be fully simulated by a rigid band model, as the  $\pi$  antibonding states appear to be quite sensitive to Al substitution, and absorb much of the added electrons. Transport properties show a substantial two-dimensionality of these compounds, due to  $\pi$  states.

We studied  $\text{CaSi}_2$  in its trigonal structure, and show that the distortion can be removed only by subtracting (in a virtual crystal-like approximation) at least 0.7 electrons. In fact,  $\text{CaBe}_{0.5}\text{Si}_{1.5}$  shows no tendency towards trigonal distortion, and electron states near  $E_F$  of similar bonding nature to those of  $\text{MgB}_2$ .

#### V. ACKNOWLEDGEMENTS

We thank M. Affronte and A. Gauzzi for stimulating discussions, and M. Affronte for sharing his results prior to publication. This work was partially supported by the Italian Consiglio Nazionale delle Ricerche (CNR) through the “Progetto 5% Applicazioni della supercondutività ad alta  $T_c$ ”. We dedicate this paper to the memory of Prof. Manca.

## TABLES

TABLE I. Phonon frequencies at  $\Gamma$  for the  $\text{AlB}_2$ type systems (in  $\text{cm}^{-1}$ ). Level degeneracies are shown in parenthesis.

	$\text{MgB}_2$	$\text{BeB}_2$
(2) $E_{1u}$	328	339
(1) $A_{2u}$	419	298
(2) $E_{2g}$	665	987
(1) $B_{1g}$	679	639

## REFERENCES

- [1] J. Nagamatsu, N. Nakagawa, T. Muranaka, Y. Zenitani, and J. Akimitsu Nature, (submitted).
- [2] J.S. Slusky *et al.*, (cond-mat/0102262)
- [3] B. Lorenz, R. L. Meng, C. W. Chu (cond-mat/0102264)
- [4] G.S. Burkhanov, M.I. Bychkova, V.A. Kuzmishchev, S.A. Lachenkov, Yu N. Likhanin, G.M. Leitus, N.N. Panov, Phys. Chem. of Mat. Treat. **29**, 303 (1995); E. Sirtl, L.M. Woerner, Journ. Cryst. Growth. **16**, 215 (1972).
- [5] P. Bordet, M. Affronte, S. Sanfilippo, M. Núñez-Regueiro, O. Laborde, G.L Olcese, Appl. Phys. Lett. (submitted).
- [6] S. Sanfilippo, H. Elsinger, M. Núñez-Regueiro, O. Laborde, S. LeFloch, M. Affronte, G.L. Olcese, and A. Palenzona, Phys. Rev. B **61**, R3800 (2000); P. Bordet et al. *ibid* **62**, 11392 (2000).
- [7] M. Affronte, O. Laborde, G.L. Olcese and A. Palenzona, J. of alloys Compounds **274** (1998) 68-73xs
- [8] I.I. Tupitsyn, Sov. Phys. Solid State **18**, 1688 (1976); ; R.C. Linton, Thin Solid Film **20**, 17 (1974); S.H. Liu, L. Kopp, W.B. England and H.W. Myron, Phys. Rev. B **11**, 3463 (1975).
- [9] I.I. Tupitsyn, I.I. Lyakovskaya, M.S. Nakhmanson, and A.S. Sukhikh, Sov. Phys. Solid State **16**, 2015 (1975).
- [10] D.R. Armstrong, A. Breeze, and P.G. Perkins, J. Chem. Soc. Faraday Trans. I, **73**, 952 (1977)
- [11] J.E. Hirsch, (cond-mat/0102115)
- [12] S. Massidda, Ph. D. thesis, ISAS-SISSA, Trieste (1985). S. Massidda and A. Baldereschi, unpublished. A. J. Freeman, A. Continenza, M. Posternak, and S. Massidda, in *Surface Properties of Layered Structures*, ed. G. Benedeck, (Kluwer, Netherlands).
- [13] S. Massidda, A. Baldereschi, Solid State Commun. **66**, 855 (1985).
- [14] T. Fauster, F.J. Himpsel, J.E. Fischer and E. W. Plummer, Phys. Rev. Lett. **51**, 430 (1983).
- [15] M. Posternak, A. Baldereschi, A.J. Freeman, and E. Wimmer, Phys. Rev. Lett. **52**, 863 (1984).
- [16] J. Kortus, I.I. Mazin, K.D. Belashchenko, V.P. Antropov, and L.L. Boyer, (cond-mat/0101446)
- [17] K.D. Belashchenko, M. van Schilfagaarde, and V.P. Anisimov, (cond-mat/0102290).
- [18] J.H. Weaver, A. Franciosi, V.L. Moruzzi, Phys. Rev. B **29**, 3293 (1979)
- [19] S. Fahy, and D.R. Hamann, Phys. Rev. B **41** 7587, (1990)
- [20] O. Bisi, L. Braichovic, C. Carbone, I. Lindau, A. Iandelli, G.L. Olcese, A. Palenzona, Phys. Rev. B **40**, 10194 (1989)
- [21] K. Kusakabe, Y. Tateyama, T. Ogitsu and S. Tsuneyumi, *Rev. of High Pressure Sci. Technol.* **7**, 193 (1998)
- [22] H.J.F. Jansen and A.J. Freeman, Phys. Rev. B **30**, 561 (1984); M. Weinert, H. Krakauer, E. Wimmer and A.J. Freeman, *ibid.* **24**, 864 (1981).
- [23] H.J. Monkhorst and J.D. Pack, Phys. Rev. B **13**, 5188 (1976).
- [24] The ABINIT code is a common project of the Universite Catholique de Louvain, Corning Incorporated, and other contributors (URL <http://www.pcpm.ucl.ac.be/abinit>).

- [25] S. Baroni, P. Gianozzi, and A. Testa, Phys. Rev. Lett. **58**, 1861 (1987).
- [26] X. Gonze, Phys. Rev. B **55**, 10337 (1997) ; X. Gonze and C. Lee, Phys. Rev. B **55**, 10355 (1997).
- [27] N. Troullier, and J.L. Martins Phys. Rev. B **43**, 1993 (1991)
- [28] S.G. Louie, S. Froyen and M.L. Cohen, Phys. Rev. B **26** 1738 (1982)
- [29] Acta Cryst. **14**, 309 (1961).
- [30] N.V. Vekshina, L.Y. Markovskii, Y.D. Kondrashew, and T.K. Voevodskaya, Z. P. K.H.A., **44**, 970 (1971)
- [31] N. Hamada, S. Massidda, Jaejun Yu, A. J. Freeman, Phys. Rev. B **42**, 6238 (1990), and references therein.
- [32] W.N. Kang *et al.* (cond-mat/0102313).
- [33] W.B. Pearson, *Handbook of Lattice Spacing and Structures of Metals and Alloys*(Pergamon, New York, 1958)
- [34] J. Evers, J. Solid State Chem. **28**,369 (1979)
- [35] H. Nakano and S. Yamanaka, J. Solid State Chem. **108**, 260 (1994), and references therein.
- [36] N. May, W. Muellery, H. Schaefer, Zeitschrift fuer Naturforschung, Teil B. Anorganische Chemie, Organische Chemie **2**, 1947 (1977).
- [37] J.S. Slusky, *et al.* (cond-mat/0102262)
- [38] K.D. Belashchenko, M. van Schilfgaarde, V.P. Antropov (cond-mat/0102290)
- [39] Y. Takano, H. Takeya, H. Fujii, H. Kumakura, T. Hatano, K. Togano, H. Kito, H. Ihara (cond-mat/0102167)
- [40] Gabino Rubio-Bollinger, Hermann Suderow, Sebastian Vieira (cond-mat/0102242)
- [41] J.F. Morar, M. Wittmer, Phys. Rev. B **37** (1988) 2618
- [42] D.D. Sarma, W.Speier, L.Kumar, C. Carbone, A. Spinsanti, O. Bisi, A. Iandelli, G.L. Olcese, A. Palenzona,Z. Phys. B **71**,69 (1988)
- [43] C. Chemelli,M. Sancrotti, L. Braichovic, F. Ciccacci, O. Bisi, A. Iandelli, G.L. Olcese, A. Palenzona, Phys. Rev. B **40**,10210 (1989)
- [44] S. Abe, H. Nakayama, T. Nishino, S. Iida, J. Mater. Res. **12** 407 (1997)
- [45] K.J. Chang, and M.L. Cohen, Phys. Rev. B **30**, 5376 (1984)

## FIGURES

FIG. 1. Band structure of  $\text{MgB}_2$ . All the energies are referred to the Fermi level, taken as zero.

FIG. 2. Total and partial density of states (PDOS) for  $\text{MgB}_2$ .

FIG. 3. Band structure of  $\text{BeB}_2$ .

FIG. 4. Band structure of  $\text{MgB}_2$  (panel (a)) and  $\text{Mg}_{0.5}\text{Al}_{0.5}\text{B}_2$  at the experimental (panel (b)) and frozen  $\text{MgB}_2$  (panel(c)) lattice parameters.

FIG. 5. Transport properties of  $\text{MgB}_2$  and  $\text{BeB}_2$  as a function of doping in a rigid band scheme. Full and dashed lines correspond to  $\text{BeB}_2$  and  $\text{MgB}_2$  respectively. Circles (squares) indicate the  $x, y$  ( $z$ ) principal values of the plasma frequency  $\Omega_p$  (in eV), of the mean squared Fermi velocity  $v_F$  (in  $10^7$  cm/sec) and of  $R_{xyz}$  (in  $10^{-10}$  m $^3$ /C, notice that  $R_{zxy} = R_{yzx}$ ). DOS are in states/eV-cell.

FIG. 6. Band structure of  $\text{CaSi}_2$  in the ideal  $\text{AlB}_2$  (dashed lines) and trigonal (full lines) structures .

FIG. 7. Total and partial density of states (PDOS) for  $\text{CaSi}_2$  in the  $\text{AlB}_2$  (dashed lines) and in the trigonal structure (full lines).

FIG. 8. Upper pannel: total energy of  $\text{CaSi}_2$  as a function of the internal parameter  $z$ , for two different values of pressure, at the corresponding experimental lattice constants ( $a = 3.7554$  Å,  $c = 4.3951$  Å for  $P = 15.0$  GPa and  $a = 3.7668$  Å,  $c = 4.4752$  Å for  $P = 12.8$  GPa, after [5]). The experimental values of  $z$  are indicated by arrows. Lower pannel: same as above, but with Ca substituted by a virtual cation having nuclear charge  $Z = 20 + x$ . The larger experimental pressure has been used ( $a = 3.708$  Å and  $c = 4.028$  Å, the experimental value of the internal parameter is  $z = 0.448$ ). The zero of energy corresponds to the  $\text{AlB}_2$  value  $z = 0.5$ .

FIG. 9. Band structure of  $\text{CaBe}_x\text{Si}_{2-x}$  ( $x = 1$ ) in the hexagonal Brillouin zone, at experimental lattice parameters.

FIG. 10. Total and partial density of states (PDOS) for  $\text{CaBe}_x\text{Si}_{2-x}$  ( $x = 1$ ) in the  $\text{AlB}_2$  structures (see text).

Fig. 1 G. Satta et al.

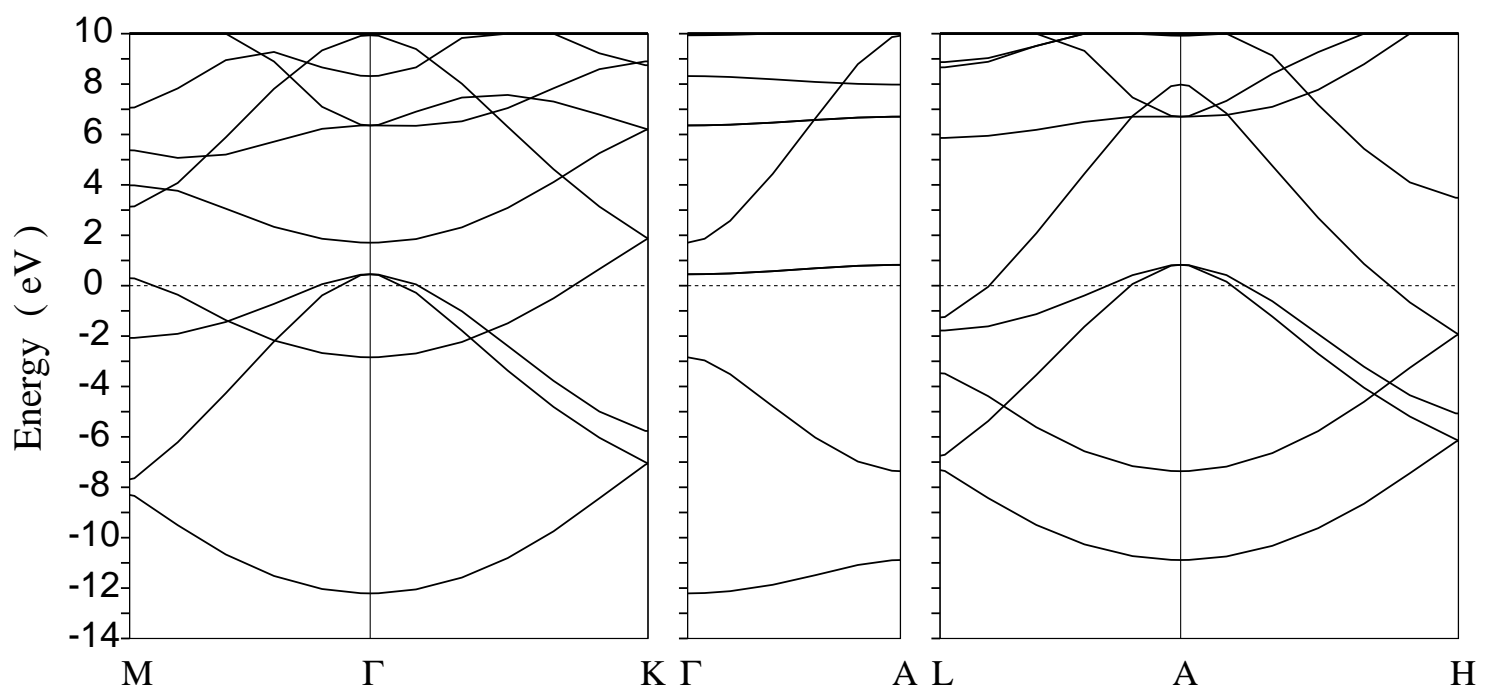
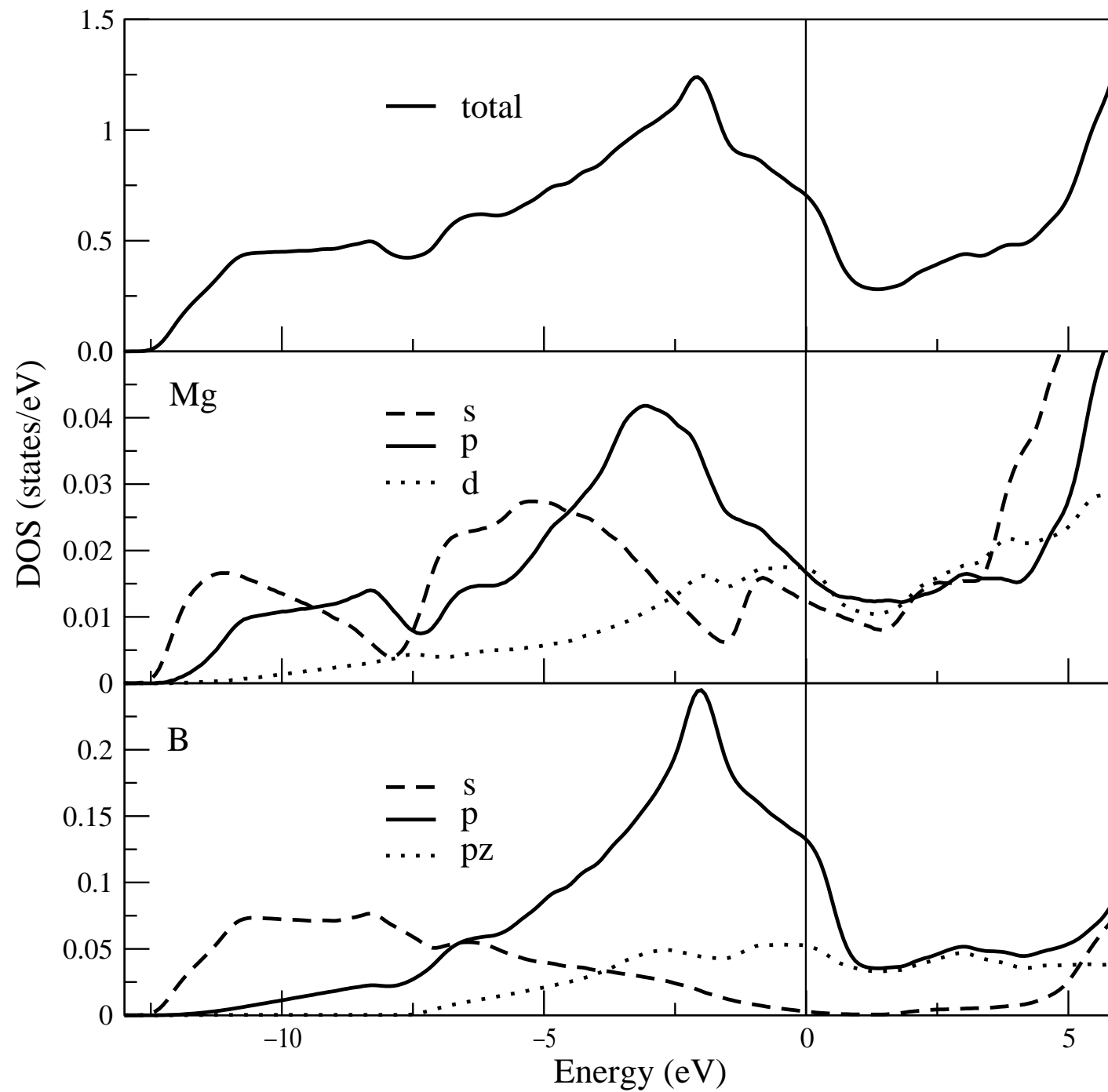


Fig. 2 G. Satta et al.



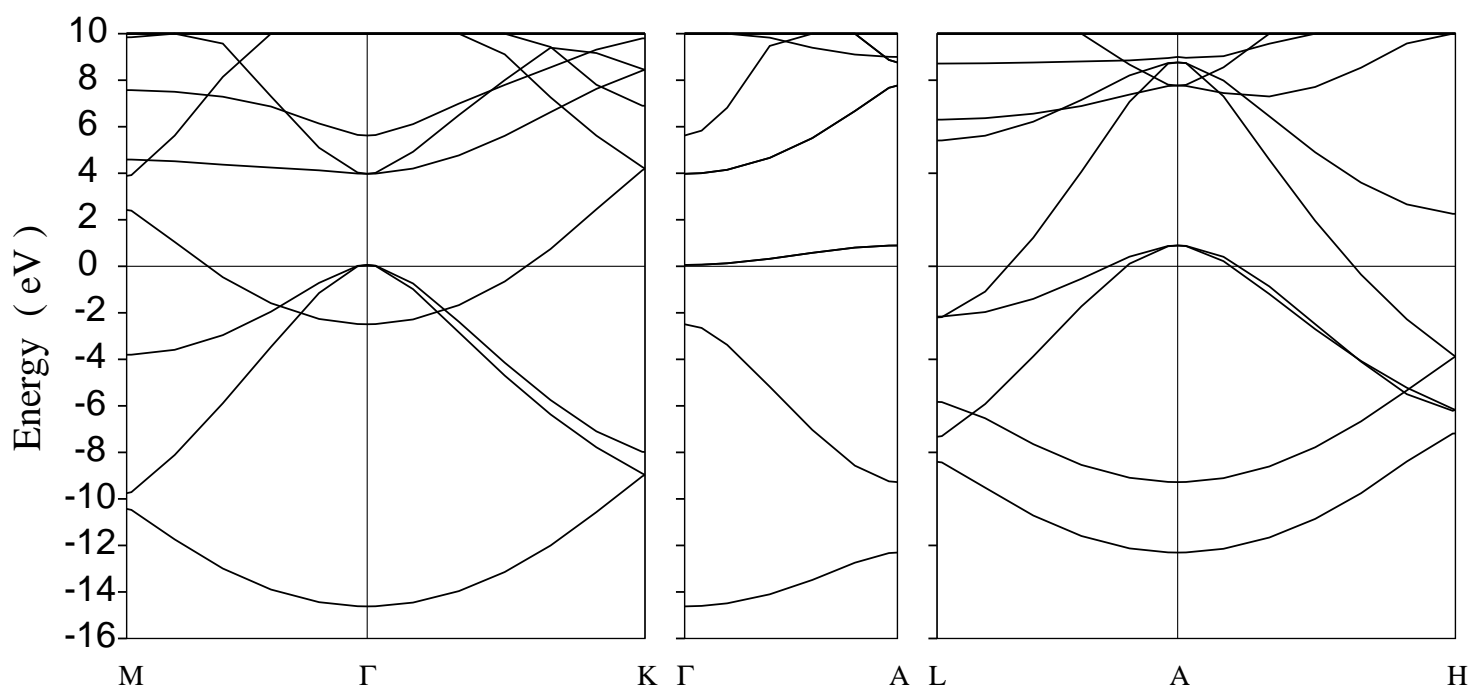


Fig. 3 G. Satta et al.

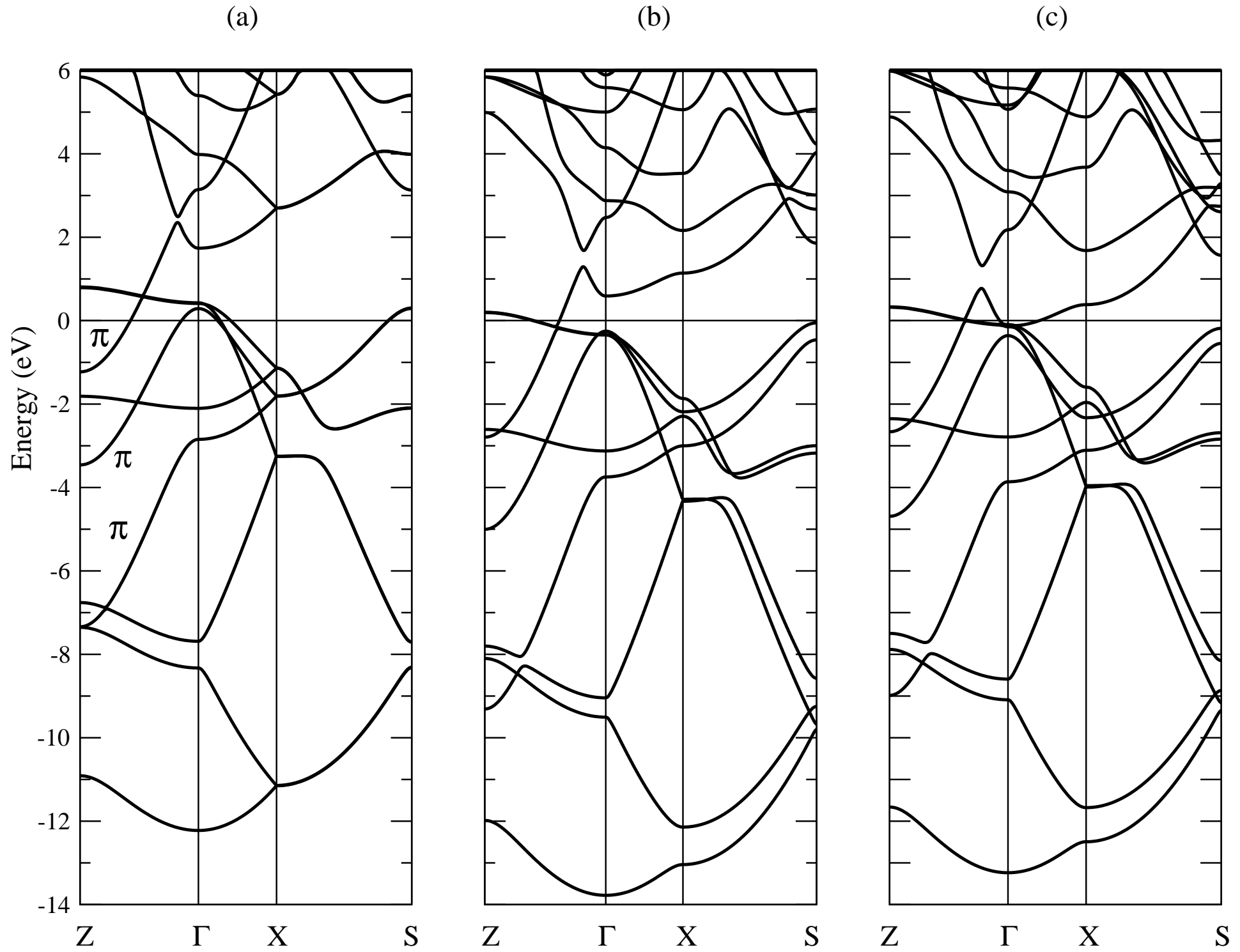


Fig. 4 G. Satta et al.

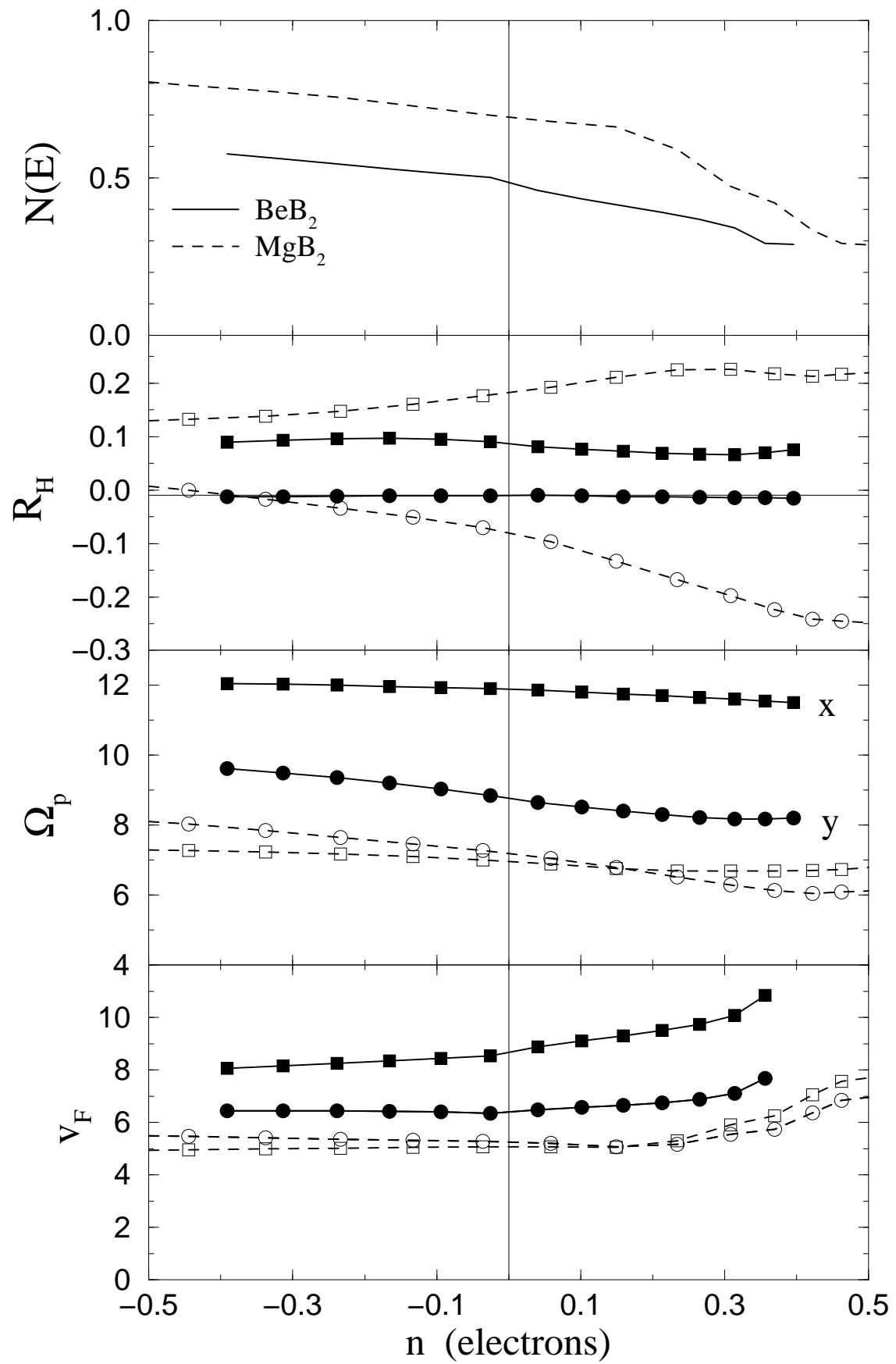
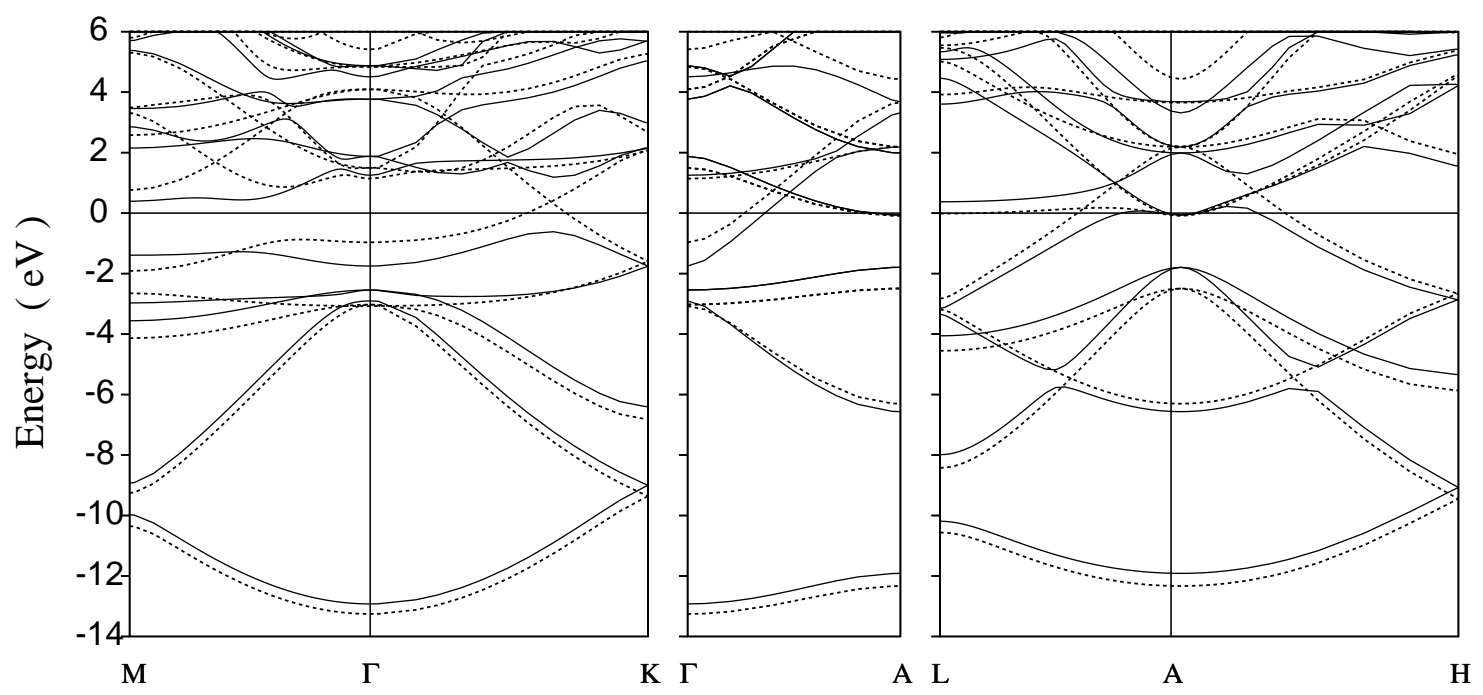


Fig. 5 G. Satta et al.

Fig. 6 G. Satta et al.



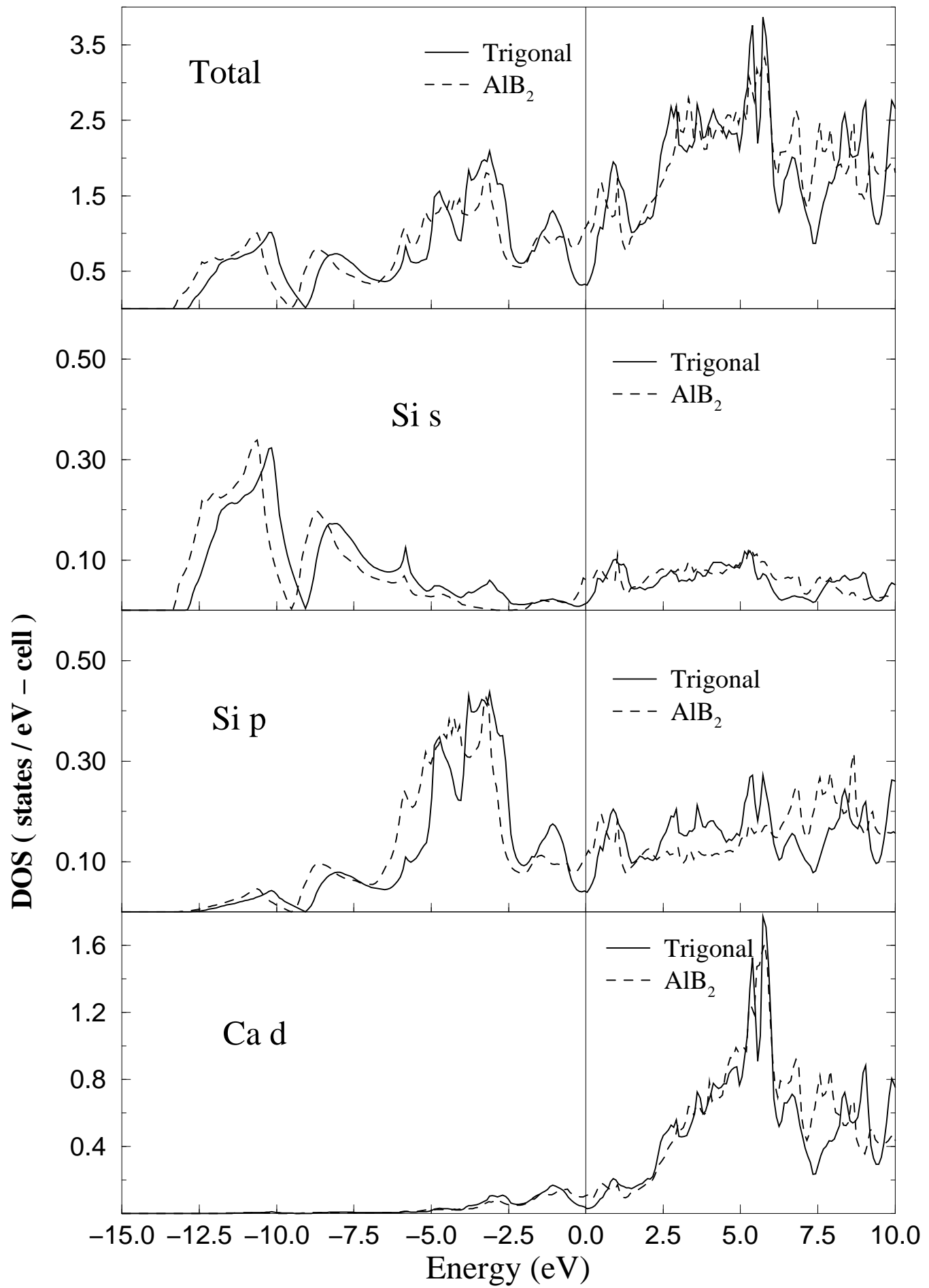


Fig. 7 G. Satta et al.

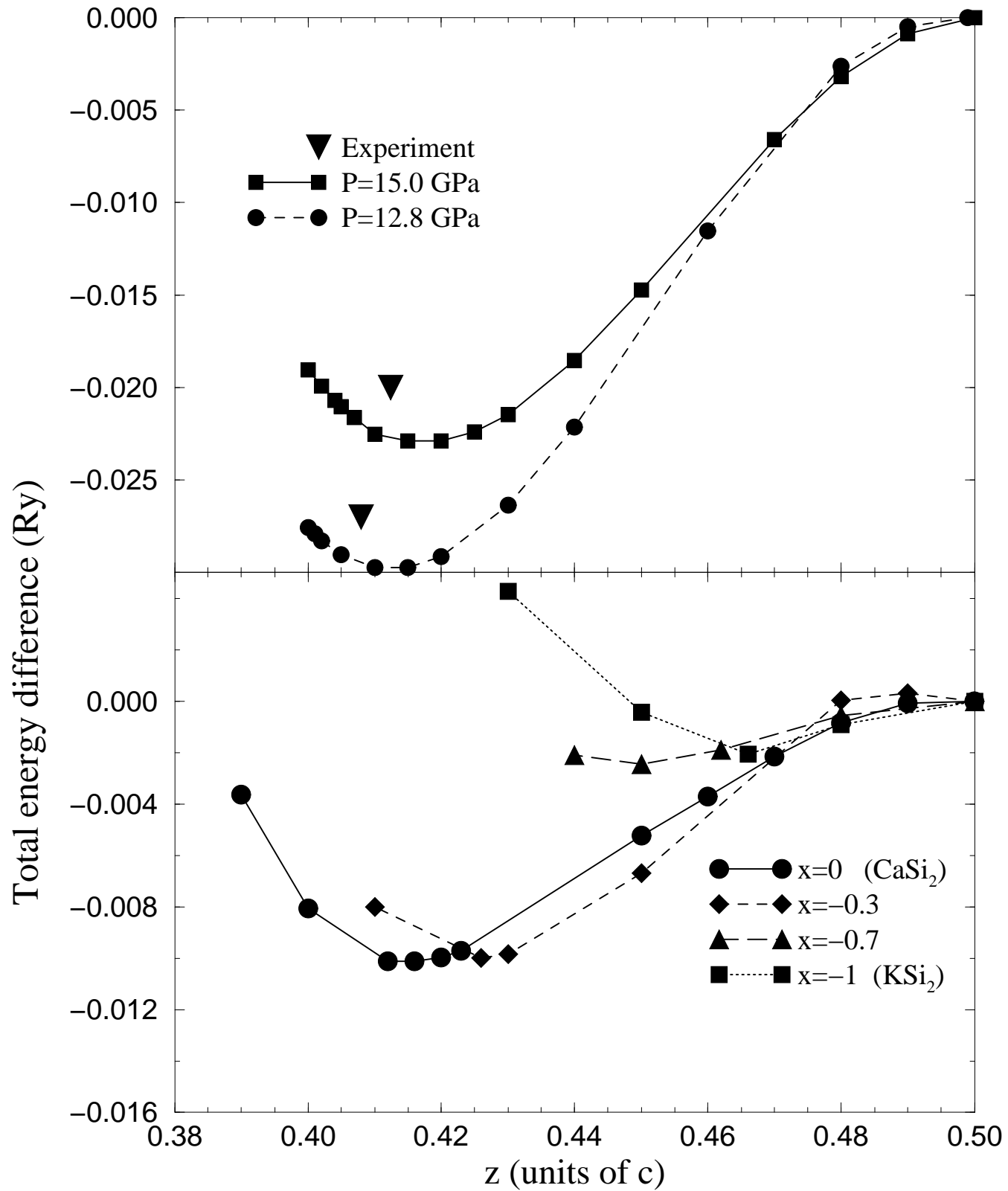


Fig. 8 G. Satta et al.

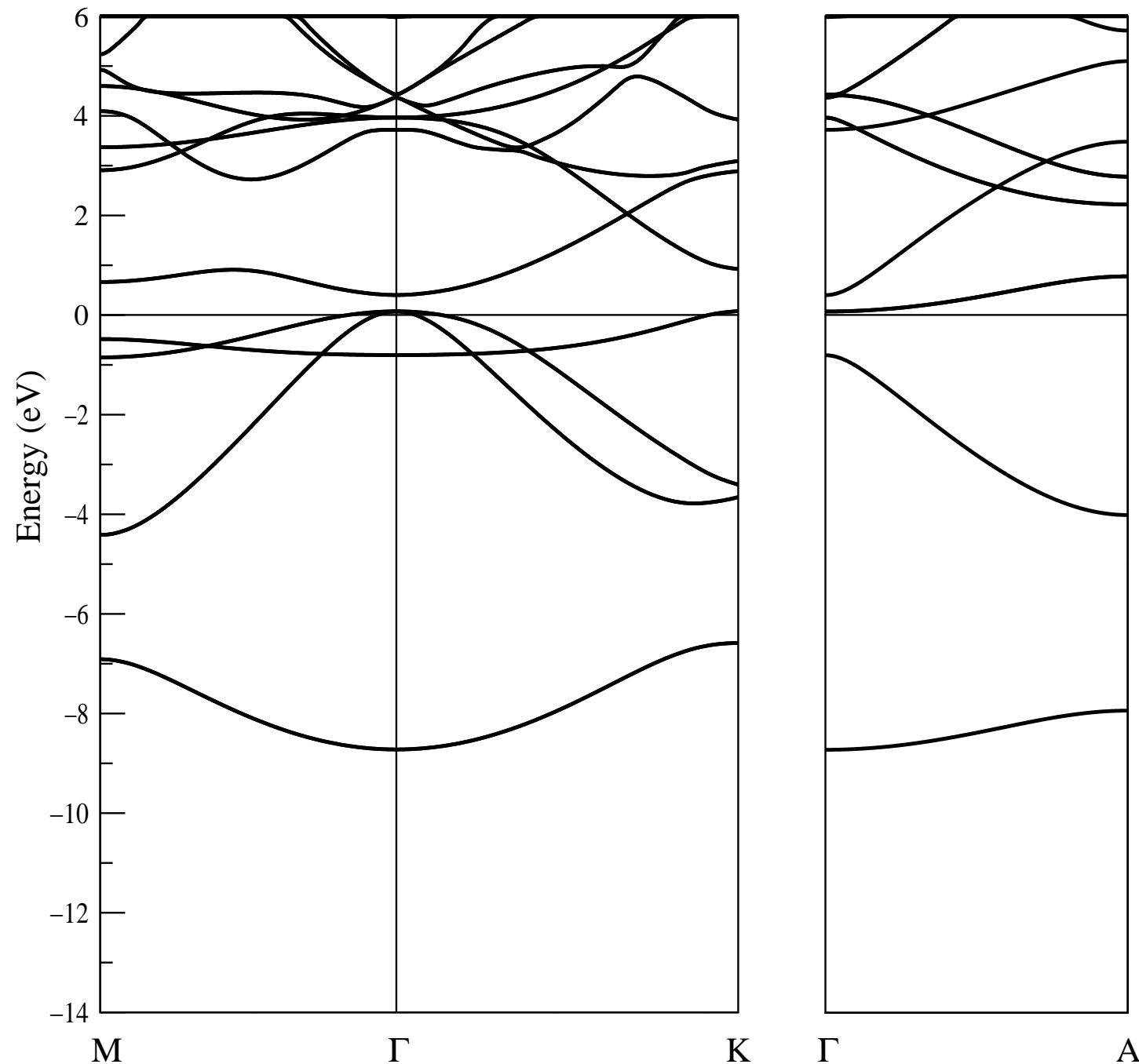


Fig. 9 G. Satta et al.

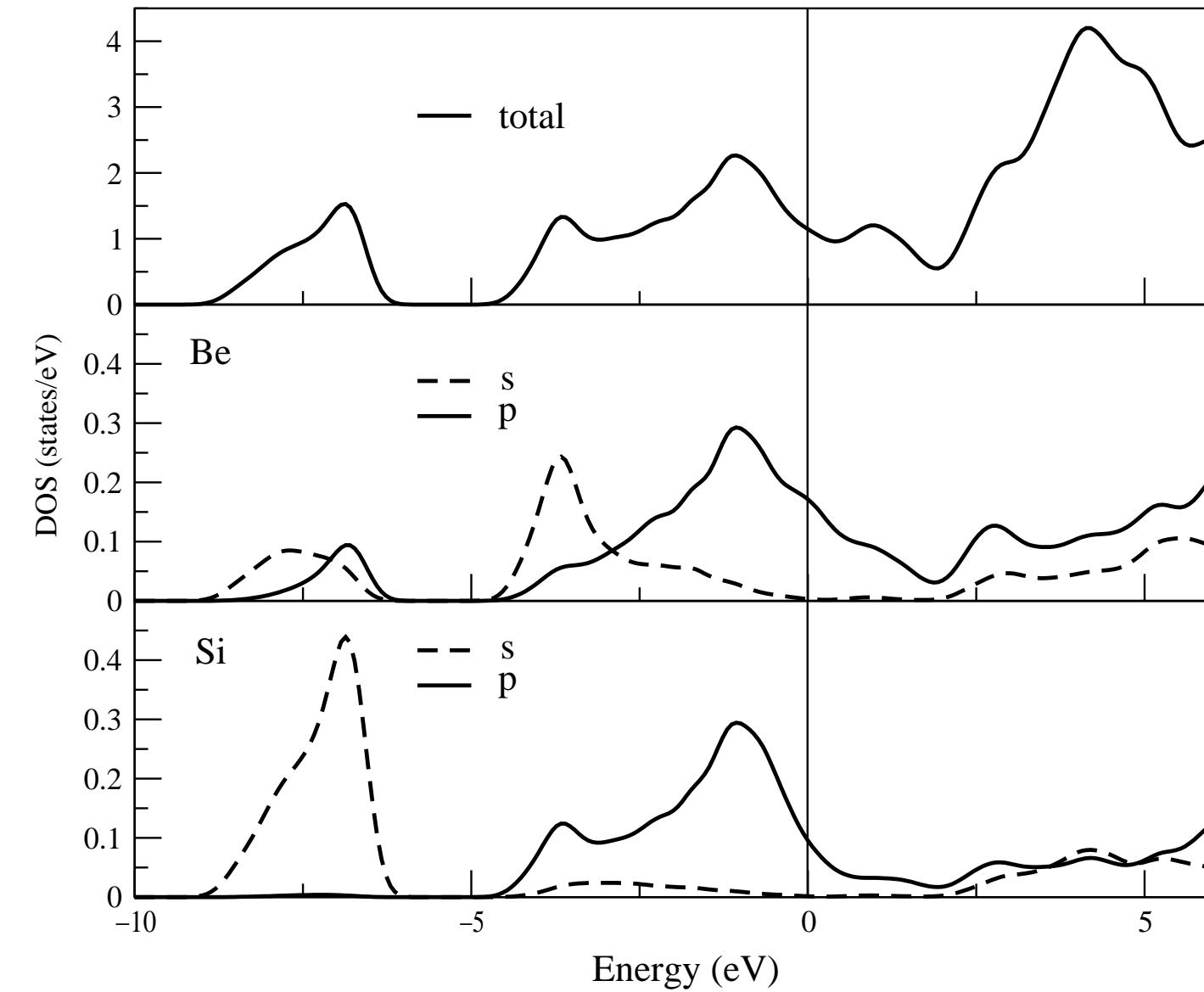


Fig. 10 G. Satta et al.